

# Experimental Investigation on Underwater Acoustic Ranging for Small Robotic Fish

Stephan Shatarra, Xiaobo Tan, Ernest Mbemmo, Nathan Gingery, and Stephan Henneberger

**Abstract**—GPS-free localization is essential for navigation and information tagging in small robotic fish-based aquatic mobile sensor networks. Constraints on size, weight, and onboard computing power, together with noisy underwater environment, have made underwater localization a particularly challenging problem. In this paper a comprehensive experimental study is presented on underwater acoustic ranging methods based on time difference of arrival (TDOA). Performances of four methods are characterized and analyzed, including threshold-crossing, tone-detection, correlation integral, and sliding-window fast Fourier transform (FFT) methods. The study facilitates the understanding of capabilities and limitations of different underwater ranging methods and provides important insight into choice of hardware and algorithms for localization of networks of small aquatic robots.

## I. INTRODUCTION

Localization without the use of Global Positioning Systems (GPS) becomes increasingly important as mobile computing devices and wireless sensor networks are getting pervasive. A number of GPS-free localization approaches have been proposed and investigated, involving the use of infrared, acoustic, ultrasonic, and radio frequency (RF) signals. Localization is typically achieved through triangulation, based on either angle of arrival (AoA) [1]–[3] or distance of travel. The distance measurement, or ranging, can be realized using the received signal strength information (RSSI) [4]. RADAR [5] and SpotOn [6] are two examples of RF RSSI-based ranging. But it is well documented that this approach is not reliable in cluttered environments. Another major approach in ranging is to measure the time of signal propagation, such as Time of Arrival (TOA), Roundtrip Time of Flight (RTOF), or Time Difference of Arrival (TDOA). The TDOA measurement is often made for concurrently sent RF and ultrasonic (or acoustic) signals, example of which include AHLoS [7], the Cricket location-support system [8], and the Calamari system [9].

There is a growing need in underwater localization, driven by recent developments in micro and small robotic fish. It is attractive to deploy mobile sensor networks for various aquatic sensing applications, such as monitoring of aquafarms for improved productivity, monitoring of drink water reservoirs to prevent algae blooms, surveillance in

seaports, and reconnaissance in hostile waters. One such sensing platform is the centimeter-scale biomimetic robotic fish propelled by electroactive polymers, developed by Tan *et al.* [10]. Having onboard localization system is essential for successful navigation of the robot and for effective coordination of robotic fish network (e.g., generation of schooling behaviors). For these systems, GPS signals are often unavailable (underwater), and even if they are available, the positioning resolution is typically inadequate.

While underwater localization and its related topics have been studied for almost a century [11]–[14], it remains challenging to perform onboard localization for small underwater robots (in this paper, by “small”, we mean the order of 10 cm or less). First, comparing to in-air localization, underwater localization itself is much more difficult. RF signals have large attenuation in water. Sound travels at about five times the speed as it does in air, which implies five times error in time-of-flight ranging methods assuming the same error in measuring the time of flight. The influence of currents, depth, temperature and salinity on sound speed [15] inevitably introduces error in estimation of travel time of the acoustic signal. Second, the speed (typically under 10 cm/s) and the size of the robotic fish demand high resolution in localization. Desired localization resolution should be at the order of 10 cm or less. Finally, the constraints on power, size, and weight require that the onboard localization system should have minimal volume and computational complexity. One should note in particular the last two points: while sonar is a mature, routine technology for submarines, the ranging/localization resolution requirement is much more relaxed, and there is virtually no constraint on the power/size of acoustic transmitters or receivers. Work related to this paper can be found in [16]; however, the authors used powerful hydrophones as transceivers and full-fledged computer systems for signal analysis, both of which will be unavailable for small, autonomous robotic fish.

This paper addresses the aforementioned challenges by experimentally investigating the capabilities and limitations of underwater localization methods for robotic fish equipped with small, lower-power sounder (buzzer) and microphones. The emphasis is placed on TDOA-based ranging as it is a key element in localization. Four methods are studied and compared for obtaining TDOA: threshold-crossing, tone-detection, correlation integral, and sliding-window fast Fourier transform (FFT). The first two methods have already been fully implemented on the existing biomimetic robotic fish, and online tracking experiment has also been conducted using the tone-detection method when the fish is tugged in

This work was supported in part by an NSF CAREER grant (ECS 0547131) and MSU IRGP (05-IRGP-418).

S. Shatarra, X. Tan, E. Mbemmo, N. Gingery, and S. Henneberger are with the Smart Microsystems Laboratory, Department of Electrical and Computer Engineering, East Lansing, MI 48824, USA (shataras@msu.edu (S. S.), xbtan@msu.edu (X. T.), mbemmoer@msu.edu (E. M.), gingeryn@msu.edu (N. G.), hennebel@msu.edu (S. H.))

Send correspondence to X. Tan. Tel: 517-432-5671; Fax: 517-353-1980.

a swimming pool. The correlation integral and FFT methods are examined on a computer using data collected from the robotic fish hardware. While requiring more computational power than the first two methods, they show great promise in achieving acceptable ranging resolution. Both methods can be implemented onboard the fish with an upgraded microcontroller, which is work underway.

The remainder of the paper is organized as follows. Section II describes the biomimetic robotic fish and its hardware for localization. In Section III through Section VI, all four methods of ranging are discussed respectively. Concluding remarks are provided in Section VII.

## II. DESCRIPTION OF ROBOTIC FISH AND LOCALIZATION HARDWARE

Fig. 1 shows the robotic fish used in this study. It is an upgraded version from that reported in [10]. The fish is propelled by an ionic polymer-metal composite (IPMC) actuator. IPMC is a class of electroactive polymers that generate large bending movement under a low actuation voltage (several volts) [17]. The IPMC actuator is further covered by a passive fin to enhance propulsion. The rigid shell of the robot was custom-made based on the shape of a real fish. It houses rechargeable batteries, a microcontroller (PIC16F688, Microchip), a Zigbee-standard RF wireless communication chip (XB24, Maxstream), a temperature sensor, and accessory circuit components such as voltage regulators, MOSFETs, filters, and amplifiers. All these components are contained in a water-proof packaging with necessary wires and pins exposed for charging batteries and driving IPMC actuator. Without the tail, the fish measures 14.8 cm long, 6.3 cm high, and 5.2 cm wide. The tail is about 5 cm long. The total weight of the robotic fish is about 140 g.

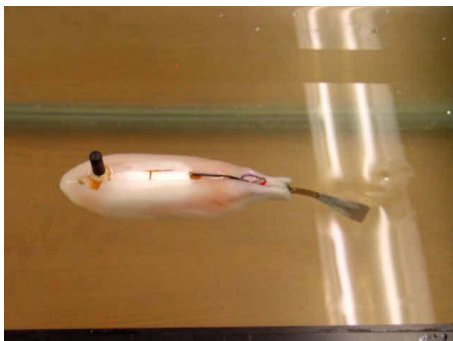


Fig. 1. The biomimetic robotic fish propelled by an ionic polymer-metal composite caudal fin.

The onboard circuit also has interface to a buzzer (CPE-267, CUI Inc.) and to a microphone (MR-23793, Knowles Acoustics) for localization purposes. These products (not shown in Fig. 1) have been chosen based on their water-proof packaging, small sizes, and light weights. The buzzer produces a sound signal of about 2.8 kHz upon activation. Ultrasonic transducers are not used due to their directivity [8], which would create blind spots for robotic fish. One pair of buzzer and microphone is currently considered for each robotic fish for sending and detecting sound waves. This

will allow ranging measurement between a robotic fish and a fixed beacon or between fish, and thus enable localization with respect to fixed, known locations or relative localization among fish nodes. Note that for navigation purposes, one also needs to know the orientation (or relative orientation) of each fish. While this could be addressed by using two pairs of buzzer/microphone and exploiting differential transmitting/detecting techniques [16], the small size of the fish relative to the acoustic wavelength (about 60 cm) makes the approach difficult. Instead, an electronic compass will be used for measuring fish orientation. Therefore, this paper will be focused on localization and in particular, ranging, only.

The ranging is based on the Time Difference of Arrival (TDOA) between an RF signal and an acoustic signal. As the RF signal propagates much faster than the acoustic one, its travel time is assumed to be zero. Each robotic fish or a fixed beacon is equipped with a buzzer, a microphone, a microcontroller, and a Zigbee chip, as described earlier (the last two also perform other control and communication functions). As RF signals propagate poorly underwater, an antenna is placed in air at the back of the fish (Fig. 1). The ranging is carried out as follows:

- Step 1: Node 1 transmits an RF packet to Node 2 to indicate it is ready;
- Step 2: Node 2 simultaneously transmits an RF packet and an acoustic pulse;
- Step 3: Node 1 receives the RF packet and starts on-board timer;
- Step 4: Node 1 receives the acoustic pulse and stops on-board timer;
- Step 5: Distance between receiver and transmitter is estimated from the timer reading.

While the protocol about seems straightforward, it is very challenging to determine the precise moment that an acoustic signal arrives (Step 4) due to various noises, multi-path effects, and hardware constraints. It is precisely this problem the paper aims to address. The four sound-arrival detection methods to be discussed later all start with the signal  $V_{mic}$ , which is obtained after the raw microphone signal passes an onboard amplifier and band-pass filter; see Fig. 2.

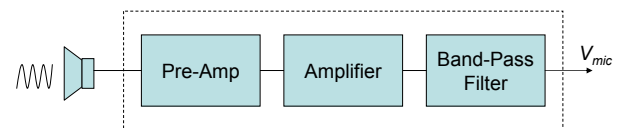


Fig. 2. Onboard preprocessing of microphone signal.

In order to understand general characteristics of the acoustic signal,  $V_{mic}$  is recorded using a Linux-based real-time control station with a sampling frequency of 49.7 kHz, for a buzzer-microphone separation of 30 cm (in air). In Fig. 3, the dashed line indicates when the acoustic signal was activated at the buzzer, while the solid line represents  $V_{mic}$ . As expected, there should be a set travel time between transmitting the acoustic pulse and receiving it. For 30 cm-separation, this should be 0.869 ms (with speed of sound in air taken

to be 345.18 m/s at  $T = 23^\circ\text{C}$ ). A closer look at 0.869 ms shows that the received signal looks like background noise. In fact a signal starts to show up after around 1.24 ms, a difference of 0.371 ms that can be explained by transient times of the buzzer and the microphone for them to reach the steady-state. More experiments have shown that the transient times are roughly constant and can be compensated during ranging. In actual ranging, delay also occurs due to RF transmitting/receiving and microcontroller operations, which has been experimentally characterized to be 6.59 ms and compensated in range calculation.

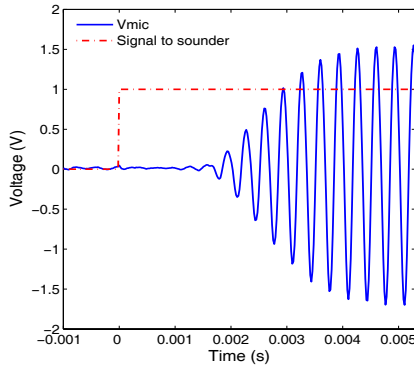


Fig. 3. Typical microphone signal in relation to activation of the sounder (separation: 30 cm).

### III. RANGING BASED ON THRESHOLD-CROSSING

The simplest method for detecting the arrival of acoustic signal is to compare  $V_{mic}$  against a threshold value.  $V_{mic}$  was fed into two on-board comparators, both internal to the microcontroller. One comparator is set up with a positive threshold (with respect to the average DC value of  $V_{mic}$ ), while the other with a negative threshold. Once  $V_{mic}$  exceeds either threshold, the on-board timer is stopped.

Both in-air and underwater experiments were conducted, partly to understand the difference between in-air and underwater ranging. In-air experiments were run in a eight by eight meter room, cluttered with laboratory equipment and other lab members. Data was collected for different distances  $L$ , specifically, every 20 cm starting from 40 to 200 cm. At each distance, 20 acoustic pulses were sent, each lasting 20 ms with a 30 ms silent interval between pulses. Note that multiple data points were collected at each distance to minimize the effect of random noises. A threshold of  $\pm 100$  mV was used. Fig. 4 shows the ranging results, both the raw data and their medians and averages at each distance. Clearly the median curve provides much more consistent result since it effectively eliminates the impact of outliers. The ranging error was found to be about 2 cm, which is comparable to the state of the art reported in literature for in-air ranging. Ranging in air beyond 200 cm was not pursued further as the main goal was to investigate underwater localization.

Underwater experiments were performed in a 25 by 10 yard swimming pool, with depth varying from 4 feet in one end to 10 feet in the other end. Swimmers were not

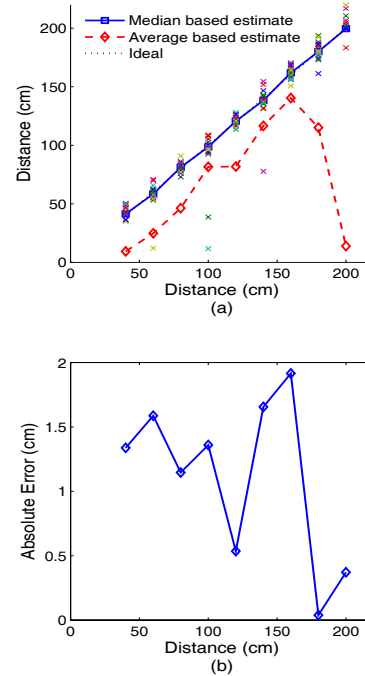


Fig. 4. Experimental results on ranging in air using threshold crossing. (a) Estimated distances based on average and median of data points; (b) ranging error based on median of data points.

present when the data were collected; however, constantly running pool filtration system contributed noises. As seen from Fig. 5, the noise underwater is much higher than in air. The threshold in sound wave detection was raised to  $\pm 600$  mV. Beyond 500 cm, the signal was barely distinguishable from the noise. Again, the median curve of data points provides more consistent ranging result, with a maximum ranging error of about 90 cm over 500 cm range. This clearly illustrates the difference between in-air and underwater acoustic ranging. Another interesting observation from Fig. 5 is that the empirical ranging curve (median-based) appears to be nonlinear. This is likely due to the nonuniform depth of the pool, which leads to varying propagation speed of the sound [15].

### IV. RANGING BASED ON TONE DETECTION

The second method uses a tone detector chip (LMC567, National Semiconductor) tuned to 2.8 kHz, with  $V_{mic}$  as its input. The output is connected to the onboard microcontroller. The output remains at the positive voltage-supply rail as long as no signal is detected. Once the internal phase locked loop (PLL) is locked, the output is switched to ground, at which point the timer is stopped.

The experiment was run underwater, with 20 data points collected at each distance. The experimental results are shown in Fig. 6. Comparing to the threshold-crossing method, the approach is more robust to noises and the median-based curve and the average-based one almost overlap. It can cover almost double the range of the threshold-crossing method. The problem with tone detection, however, is the uncertainty in time it takes for the internal PLL to

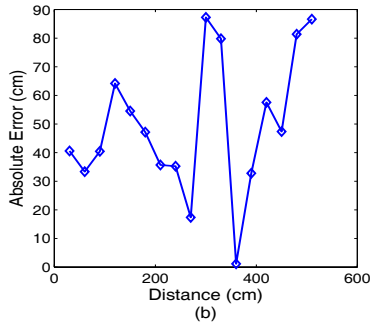
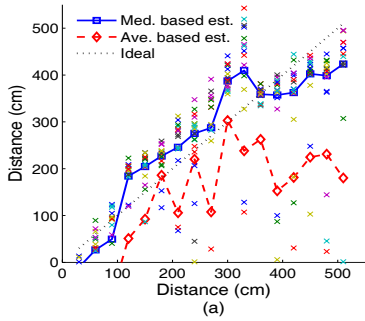


Fig. 5. Experimental results on ranging underwater using threshold crossing. (a) Estimated distances based on average and median of data points; (b) ranging error based on median of data points.

lock on. Considering the wavelength of sound underwater, a ranging error of more than 50 cm will be introduced for one missed cycle in PLL. Furthermore, it is assumed that the frequency of the sounder is constant. This is not the case; experimental data showed a standard deviation of 90.4 Hz, which affects the lock-on time. From Fig. 6, the ranging error is mostly under 130 cm (maximum 180 cm) over about 1000 cm. Percentage-wise, this is comparable to the threshold-crossing method. Interestingly, Fig. 6 seems to confirm the nonlinear range function observed also in Fig. 5.

A localization experiment was further performed using the tone-detection method. As shown in Fig. 7, the robotic fish was manually tugged through the pool with a microphone tied to the bottom of the fish. Tugging the fish was decided instead of letting the fish swim by itself, since the pool current due to filtration processing would push the fish off a straight line and create difficulty for validating the localization method. Two buzzers were attached underwater to the wall of the pool at each end. Localization took place every 20 seconds, for six locations. For each location, 10 pulses (each lasting 20 ms with 30 ms silence in between) were sent by one buzzer and then 10 pulses sent by the other buzzer, which took a total of 1 second. Fig. 8 shows the result of localization for two runs. It can be seen that the onboard tone-detection can approximately track the position of the robot, with an error commensurate with that in Fig. 6.

## V. RANGING BASED ON CORRELATION INTEGRAL

In order to improve ranging accuracy, we have further explored two methods that require more intensive processing of the signal  $V_{mic}$  (this section and Section VI). For both

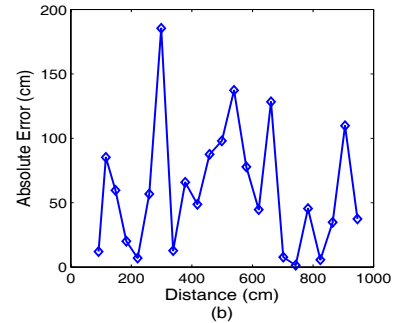
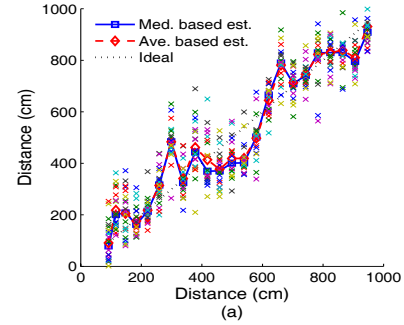


Fig. 6. Experimental results on ranging underwater using tone detection. (a) Estimated distance versus actual distance; (b) ranging error based on median of data points.

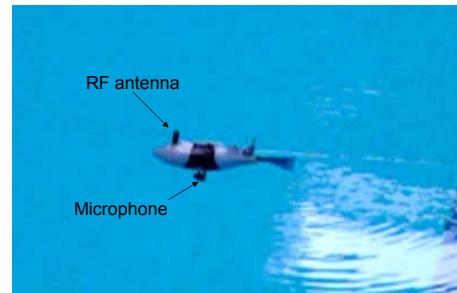


Fig. 7. Localization experiment in a swimming pool.

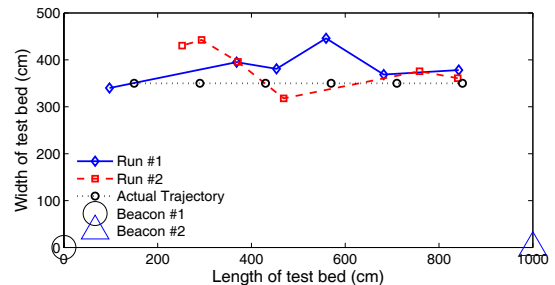


Fig. 8. Experimental results on localization based on tone-detection. methods, as proof of concept,  $V_{mic}$  was recorded using a data acquisition card and then processed in a computer to calculate the arrival time of sound. Both methods will be

implemented onboard the fish after moderate upgrading of the processing hardware.

The correlation integral method is based on integrating the product of  $V_{mic}$  and a sinusoidal signal  $\sin(\omega t)$ , where  $\omega$  denotes the frequency of the acoustic signal. In particular, once the receiving node gets the RF packet, it starts to compute  $\int_0^t V_{mic}(\tau) \sin(\omega \tau) d\tau$ . Suppose the distance is  $L$ . Let  $v$  denote the sound speed. Then under an ideal condition,  $V_{mic}(t)$  can be expressed as

$$V_{mic}(t) = \begin{cases} 0 & \text{if } t \leq \frac{L}{v} \\ A(L) \left(1 - e^{-\frac{t-L/v}{T}}\right) \sin(\omega t + \frac{\omega L}{v} + \phi) & \text{if } t > \frac{L}{v} \end{cases}, \quad (1)$$

where  $A(L)$  represents the steady-state amplitude of  $V_{mic}$ , which is a function of  $L$ , and  $\phi$  denotes the (unknown) phase of the original signal at the buzzer.  $T$  represents the time constant of the buzzer/microphone transient dynamics; refer to Fig. 3. Letting  $\theta \triangleq \omega L/v + \phi$ , one can show, when  $t \leq \frac{L}{v}$ , the integral signal  $I(t) = \int_0^t V_{mic}(\tau) \sin(\omega \tau) d\tau = 0$ , and when  $t > \frac{L}{v}$ ,

$$\begin{aligned} I(t) = & \frac{A(L) \cos(\theta)}{2} \left(t - \frac{L}{v}\right) - \frac{A(L)}{4\omega} \sin(2\omega t + \theta) \\ & + \frac{A(L)T \cos(\theta)}{2} \left(e^{-\frac{t-L/v}{T}} - 1\right) + \frac{A(L)}{4\omega} \sin\left(\frac{2\omega L}{v} + \theta\right) \\ & + \frac{2\omega}{4\omega^2 + T^2} e^{-\frac{t-L/v}{T}} \left(\sin(2\omega t + \theta) - \frac{T}{2\omega} \cos(2\omega t + \theta)\right) \\ & - \frac{2\omega}{4\omega^2 + T^2} \left(\sin(2\omega L/v + \theta) - \frac{T}{2\omega} \cos(2\omega L/v + \theta)\right). \quad (2) \end{aligned}$$

Despite the complex looking of (2), only the first two terms will persist as others will vanish due to the exponential decaying. This implies that, when  $t > \frac{L}{v}$ ,  $I(t)$  will be approximated by a linearly growing term superimposed by a low-amplitude, high frequency sinusoidal signal. Fig. 9 illustrates the analysis above, where one can see the integral curve consists of roughly the superposition of a linearly decaying signal and a small oscillatory signal. The time of travel can be inferred from the time instant  $t$  when  $I(t)$  starts to deviate from 0, and in practice, deviate beyond certain threshold.

Fig. 10 shows the experimental results on ranging using correlation integral, where 14 acoustic pulses were sent and collected for each location. Significant improvement can be seen over the previous two methods: a maximum ranging error of 45 cm over the range of 6 m. The remaining error is due to the difficulty in proper choice of the threshold, which is a constant tradeoff problem between false alarm and mis-detection.

## VI. RANGING BASED ON SLIDING-WINDOW FFT

The last method studied involves FFT analysis for a sliding window of sampled  $V_{mic}$  signals. In the experiment, the sampling frequency is 49.7 kHz. A window with length 35 samples is adopted, which represents roughly two periods of the acoustic signal. FFT is performed recursively since only one sample is different for two consecutive windows. The algorithm then looks for the frequency component corresponding to the acoustic signal. When its magnitude is

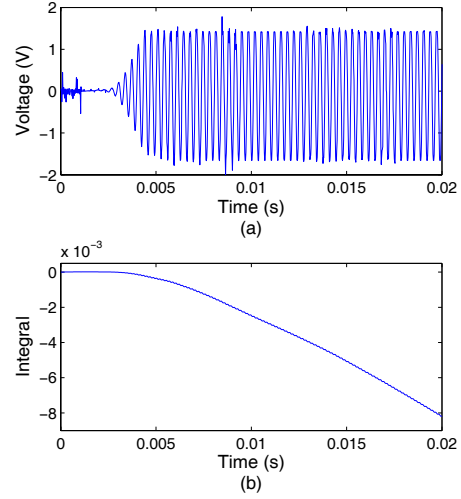


Fig. 9. Illustration of the integral method. (a) Example of  $V_{mic}$ ; (b) correlation integral.

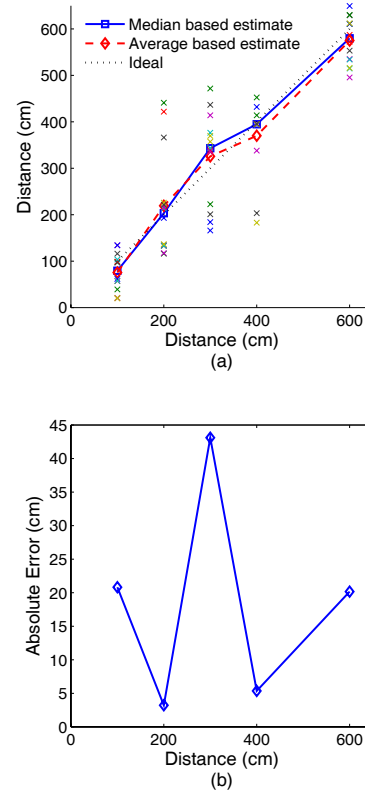


Fig. 10. Experimental results on ranging underwater using correlation integral. (a) Estimated distance versus actual distance; (b) ranging error based on the median curve.

higher than a set threshold, the acoustic signal is considered to have arrived. The sample number of the start of the present window is recorded and translated to time. Fig. 11 shows the ranging result based on the FFT method, where 14 acoustic pulses were used at each location. From the figure, this approach can achieve 25 cm ranging precision for a range of 8 m, which is the highest among all methods studied in this paper.



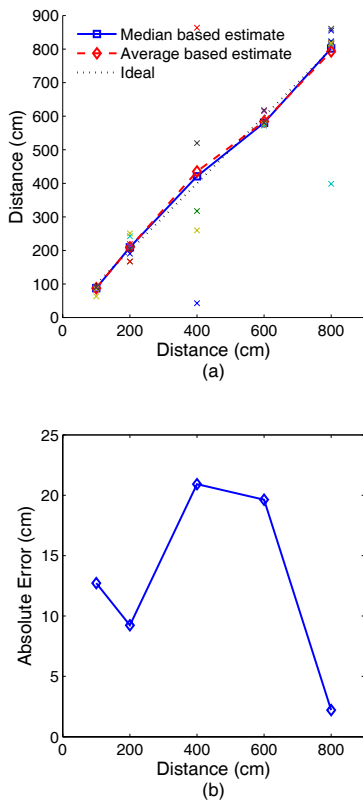


Fig. 11. Experimental results on ranging underwater using sliding-window FFT. (a) Estimated distance versus actual distance; (b) ranging error based on the median curve.

TABLE I  
SUMMARY OF FOUR RANGING METHODS

Methods	Range	Accuracy	Complexity
Threshold	Small	Low	Low
Tone-detect	Large	Low	Low
Integral	Medium	High	Medium/High
FFT	Large	High	High

## VII. CONCLUSIONS

In this paper, comprehensive experimental investigation of ranging methods was reported for centimeter-scale underwater robots, together with analysis on sources of ranging errors. The work was motivated by the need to localize such robots for mobile sensing applications, under the requirement of high localization precision yet with severe constraints on hardware/software size and complexity. Capabilities and limitations of each of the four methods were examined and compared, which are summarized in Table I.

The study concludes that it is possible to achieve underwater localization resolution of 20 cm over a range of 10 m, with the small, low-power buzzer and microphone used in this paper. Work is underway to characterize the localization performance over 25 m. We are also working on onboard implementation of the correlation integral method and the FFT method. Since both algorithms can be executed recursively, onboard localization can be realized by upgrading the current microcontroller to a dsPIC-family chip by Microchip, which is capable of performing complicated computations.

The correlation integral method could also be implemented using additional circuit components.

## ACKNOWLEDGMENT

The authors would like to thank Bryan Thomas for his assistance in developing and testing the underwater ranging methods.

## REFERENCES

- [1] A. A. Handzel and P. S. Krishnaprasad, "Biomimetic sound-source localization," *IEEE Sensors Journal*, vol. 2, no. 6, pp. 607–616, 2002.
- [2] D. Niculescu and B. Nath, "Ad hoc positioning system (APS) using AOA," in *Proceedings of the Twenty-Second Annual Joint Conference of the IEEE Computer and Communications Societies (INFOCOM 2003)*, 2003, pp. 1734–1743.
- [3] P. Rong and M. L. Sichitiu, "Angle of arrival localization for wireless sensor networks," in *Proceedings of the 3rd Annual IEEE Communications Society Conference on Sensor and Ad Hoc Communications and Networks*, 2006, pp. 374–382.
- [4] K. Whitehouse, C. Karlof, and D. Culler, "A practical evaluation of radio signal strength for ranging-based localization," *ACM SIGMOBILE Mobile Computing and Communication Review*, vol. 11, no. 1, pp. 41–52, 2007.
- [5] P. Bahl and V. N. Padmanabhan, "RADAR: An in-building RF-based user location and tracking system," in *Proceedings of the Nineteenth Annual Joint Conference of the IEEE Computer and Communications Societies (INFOCOM 2000)*, 2000, pp. 775–784.
- [6] J. Hightower, C. Vakili, G. Borriello, and R. Want, "Design and calibration of the SpotON ad-hoc location sensing system," University of Washington, Tech. Rep., 2001, available at [citeseer.ist.psu.edu/479904.html](http://citeseer.ist.psu.edu/479904.html).
- [7] A. Savvides, C.-C. Han, and M. B. Strivastava, "Dynamic fine-grained localization in ad-hoc networks of sensors," in *Proceedings of the 7th Annual International Conference on Mobile Computing and Networking*, 2001, pp. 166–179.
- [8] N. B. Priyantha, A. Chakraborty, and H. Balakrishnan, "The Cricket location-support system," in *Proceedings of the 6th Annual International Conference on Mobile Computing and Networking*, 2000, pp. 32–43.
- [9] C. D. Whitehouse, "The design of Calamari: An ad-hoc localization system for sensor networks," Master's thesis, University of California, Berkeley, 2002.
- [10] X. Tan, D. Kim, N. Usher, D. Laboy, J. Jackson, A. Kapetanovic, J. Rapai, B. Sabadus, and X. Zhou, "An autonomous robotic fish for mobile sensing," in *Proceedings of the IEEE/RSJ International Conference on Intelligent Robots and Systems*, Beijing, China, 2006, pp. 5424–5429.
- [11] A. B. Wood and H. E. Browne, "A radio-acoustic method of locating positions at sea: Application to navigation and to hydrographical survey," *Proceedings of the Physical Society of London*, vol. 35, no. 1, pp. 183–193, 1922.
- [12] A. Quazi, "An overview on the time delay estimate in active and passive systems for target localization," *IEEE Transactions on Acoustics, Speech, and Signal Processing*, vol. 29, no. 3, pp. 527–533, 1981.
- [13] S. M. Smith and D. Kronen, "Experimental results of an inexpensive short baseline acoustic positioning system for AUV navigation," in *Proceedings of MTS/IEEE Conference on OCEANS*, 1997, pp. 714–720.
- [14] M. Watson, C. Loggins, and Y. T. Ochi, "A new high accuracy super-short baseline (SSBL) system," in *Proceedings of International Symposium on Underwater Technology*, 1998, pp. 210–215.
- [15] H. Medwin, "Speed of sound in water for realistic parameters," *Journal of Acoustical Society of America*, vol. 58, p. 1318, 1975.
- [16] N. Kottege and U. R. Zimmer, "Relative localisation for AUV swarms," in *Proceedings of the Symposium on Underwater Technology and Workshop on Scientific Use of Submarine Cables and Related Technologies*, 2007, pp. 588–593.
- [17] M. Shahinpoor and K. Kim, "Ionic polymer-metal composites: I. Fundamentals," *Smart Materials and Structures*, vol. 10, pp. 819–833, 2001.